Understanding the Influence of Molecular Weight on the Corrosion Inhibition Performance of Two Cellulosic Polymers

I. O. Arukalam[1*], I. C. Madufor[1], O. Ogbobe[1] and E. E. Oguzie[2]

[1]*Department of Polymer and Textile Engineering, Federal University of Technology, P.M.B. 1526 Owerri, Nigeria.*
[2]*Department of Chemistry, Electrochemistry and Materials Science Research Laboratory, Federal University of Technology, P.M.B. 1526 Owerri, Nigeria.*

Authors' contributions

This work was carried out in collaboration between all authors. Authors OO, ICM and EEO designed the study, performed the statistical analysis, wrote the protocol, and the first draft of the manuscript. Author IOA performed the experimental work, managed the literature searches and analyses of the study. All authors read and approved the final manuscript.

Original Research Article

ABSTRACT

Corrosion inhibitory efficacy of two cellulosic polymers, hydroxyethyl cellulose (HEC) and hydroxypropyl methylcellulose (HPMC) on mild steel in 1 M HCl have been investigated with a view to assessing the influence of molecular weight on the inhibition performance. In the study, weight loss measurement technique, electrochemical impedance spectroscopy and potentio-dynamic polarization corrosion monitoring techniques were employed. Weight loss results reveal that on comparative analysis, HPMC gives better inhibition performance than HEC, though both polymeric molecules achieved inhibition efficiency up to 90%. Changes in impedance and polarization parameters suggest the adsorption of HEC and HPMC on the mild steel surface, leading to the formation of protective polymeric films. Furthermore, HPMC that has larger molecular weight than HEC also showed higher adsorptive capability following thermodynamic-kinetic isotherm model.

_____

Corresponding author: E-mail: innocentarukalam@yahoo.com;

The experimental results were corroborated by results from theoretical studies which involve quantum chemical calculation and molecular dynamics simulation, whereby the HPMC molecules demonstrated higher ability to donate electrons to the vacant d-orbital of the metal, than HEC molecules.

1. INTRODUCTION

Steel structures and their alloys are frequently employed in industrial activities where their operations are chemically challenged as they come in contact with aggressive media such as acid solutions [1]. This contact more often than not results in corrosion.

Corrosion control and prevention of these steel structures are of industrial, economical, technical, environmental and aesthetic importance to the general society. Hence, the use of corrosion inhibitors has remained one of the best approaches of protecting metals and alloys against the menace of corrosion [2-4]. Unfortunately, a large number of available effective corrosion inhibitors are toxic. It is due to the toxicity of some of these organic corrosion inhibitors that the search for green corrosion inhibitors which are biodegradable, non-polluting and do not possess heavy metals or other toxic compounds has received increased attention [5-7].

Furthermore, the effectiveness of organic compounds as corrosion inhibitors has been ascribed to their functional groups, molecular structures, molecular size, molecular mass and adsorptive/film-forming capability of the compounds [8,9]. In addition to the aforementioned factors that govern the performance of organic inhibitors, some other factors are also contributory to the performance appraisal of the inhibitors and they include chain length, aromaticity/conjugation, bonding strength between the inhibitors and the corroding metals, cross-linking and solubility of the reaction environment [10-12].

The organic corrosion inhibitors have been reported to function by adsorbing on the metal surface, displacing the pre-adsorbed water molecules on the metal surface via substitution reaction and forming a protective barrier film which isolates the metal surface from the corrosive media [13,14].

It has also been reported that non-toxic hydroxyethyl cellulose and hydroxypropyl methylcellulose derivatives [15-17] and other green synthetic polymers [18,19] have proven to be good corrosion inhibitors for some metals and their alloys. However, the solubility of polymers and their consequent adsorption and corrosion inhibition is thought to follow a trend which is dependent on the bulk properties of the polymers [20].

Other authors [21-23] have also reported on the effect of molecular weight on the corrosion inhibition performance of some polymers. Reports show that the dissolution of a polymer in solvent is generally a slow process which can take several weeks depending on the structure and molecular weight of the polymer. These polymers constitute long chains with a large number of segments, forming tightly folded coils which are even entangled to each other. Numerous cohesive and attractive both intra and intermolecular forces such as dispersion, dipole-dipole interaction, induction, and hydrogen bonding hold these coils together. Based on these features, one may expect noticeable differences in the dissolution behavior shown by polymers. Due to their size, coiled shape and the attractive forces between them, higher molecular weight polymers become dissolved quite slowly than lower molecular weight polymers. This affects the instantaneous adsorption of the formed polymeric film. However, the adsorption of high molecular weight compounds such as polymer increases with time, temperature and net solubility parameters among others between the polymer and the reaction medium.

The purpose of this study is to appraise the inhibition performance and influence of molecular weight of two cellulosic polymers whose weight of one molecule calculated from the geometry optimized structure in Fig. 4 (a)i and (b)i is 184 g/mol for hydroxyethyl cellulose, (HEC) and 196 g/mol for hydroxypropyl methylcellulose (HPMC), on the mild steel corrosion in hydrochloric acid solution. Gravimetric measurement technique was used to ascertain the concentration-dependent effect of the corrosion inhibitors. Electrochemical techniques were used to study the kinetics of the

electrochemical process occurring at the metal/solution interface and the specific effect of the inhibitors in relation to anodic and cathodic reactions, while quantum chemical computational approach has been used to establish the relationship between the inhibition efficiency and molecular orbitals/electronic structure properties of the corrosion inhibitors. Molecular dynamics simulation has been employed to illustrate the adsorption behavior of the inhibitors on the metal surface.

2. Experimental

2.1 Weight Loss Measurements

The experiments were performed on mild steel specimens having the following percentage chemical composition: Si: 0.02; C: 0.05; Mn: 0.18; Cu: 0.02; Cr: 0.02 and the remainder Fe. The mild steel sheet of thickness 0.05 cm was machined into test coupons of length, 4 cm and width, 2 cm and a small hole was drilled at one end of the coupon to enable suspension into test solution in the beaker. The metal specimens were polished with fine SiC emery paper up to 800 grits, degreased and cleaned as described elsewhere [24,25]. HEC and HPMC sourced from Sigma Aldrich chemical company were used without further purification; at varying concentrations of 500, 1000, 1500 and 2000 mg/l. Blank hydrochloric acid solution was prepared in the concentration of 1 M HCl.

Weight loss experiments were conducted on test coupons under total immersion conditions in 200 ml of test solutions at ambient temperature, 29±1°C. The pre-cleaned and weighed coupons were suspended in 250 ml capacity beakers containing the test solutions, using glass rods and hooks. All tests were made in aerated solutions and were run three times to ensure good reproducibility. To determine weight loss with respect to time and additive concentrations, the coupons were retrieved from test solutions at 24-h interval, progressively for 120 hs (5 days). The corrosion rates of mild steel in 1 M HCl solution and the acid solution containing the additives, HEC and HPMC were calculated using the expression [26]:

$$\text{Corrosion rate, } R_c \text{ (mm/y)} = \left[\frac{87,600\Delta W}{\rho A t} \right] \tag{1}$$

where ΔW, ρ, A, t are weight loss in gram, density of the metal g/cm^3, surface area of the

test coupon in cm^2 and time of exposure in the test solution in hour, respectively.

The inhibition efficiency was taken to represent the surface coverage (θ), where $(\theta = IE\%/100)$. The percentage inhibition efficiency was calculated using Eq. (2):

$$IE\% = \left(\frac{Rc_o - Rc_{inh}}{Rc_o} \right) X100 \tag{2}$$

where both R_{Co} and Rc_{inh} are the corrosion rates in the uninhibited and inhibited solutions respectively.

2.2 Electrochemical Measurements

2000 mg/l concentration of the inhibitor was chosen to study the kinetics of the corrosion inhibition process as well as the cathodic and anodic partial reactions occurring in the process. The potassium iodide, KI from BDH laboratory Supplies was also used. 500 mg/l KI was prepared and used as a co-inhibitor with 2000 mg/l each of HEC and HPMC. In the electrochemical studies the coupons were machined in such a way that only 1 cm^2 surface area was exposed. Before the measurements, the samples were mirror-polished using different grade emery papers followed by washing in ethanol, acetone and finally with distilled water. Electrochemical tests were carried out in a conventional three-electrode configuration with graphite rod as counter electrode and saturated calomel electrode (SCE) as the reference electrode. The working electrode (mild steel of 1cm^2 surface area exposed) was first immersed in the test solution and after establishing a steady state open circuit potential (OCP), the impedance measurements were carried out in a *VERSASTAT 3* computer controlled electrochemical workstation. The frequency range of 10 kHz to 10 mHz with amplitude of 10 mV (RMS) using a.c. signals was used. Results were obtained as Nyquist impedance loops using Zsimpwin electrochemical software. Thereafter, the potentiodynamic polarization measurements were run in the potential range of ±250 mV at a sweep rate of 0.5 mV/s.

2.3 Theoretical Studies

Quantum chemical computations were performed using the density functional theory (DFT) electronic structure programs -Forcite and DMol^3

as contained in Materials Studio 4.0 software (Accelrys Inc.) as used elsewhere [27]. The electronic structures of HEC and HPMC on Fe surface were modeled by means of the DFT electronic structure program, DMol[3]. Electronic parameters for the simulation include restricted spin polarization using DND basis set and Perdew Wang (PW) local correlation density functional. The distribution of frontier molecular orbitals, namely, the highest occupied molecular orbital (HOMO) and lowest unoccupied molecular orbital (LUMO) were evaluated. Fe (1 1 0) was chosen to simulate the adsorption process of HEC and HPMC on mild steel surface. The molecular dynamics simulation was performed at 298 K using NVE ensemble, with a time step of 0.1 fs and simulation time of 50 ps.

3. RESULTS AND DISCUSSION

3.1 Weight Loss Measurements Results

Table 1 compares the corrosion rates of mild steel in 1M HCl using the two different inhibitors-HEC and HPMC. In the Table 1, HPMC is found to show lower corrosion rates which translates to higher inhibition efficiency. From the Table 1 also, the trend of inhibition efficiency as a function of inhibitor concentration shows that efficiency of inhibition improved with increase in the concentrations of inhibitor. This behavior can also be explained on the basis of the solubility parameter between HPMC-aqueous HCl systems which is possibly slightly higher than the polymer-polymer attraction forces. Thus, instead of forming a true solution forms a jelly-like solution (even at low concentration due to high molecular weight) which on adsorption onto the metal surface forms a stronger protective film

limiting the diffusion of the corrodent on the metal. This is evident in Fig. 1 which illustrates the inhibitive capability of the adsorption film of the polymer. However, Figs. 1 a – c reveals that HPMC inhibited mild steel dissolution more than the HEC in HCl medium. The higher inhibition efficiency of HPMC is attributed to higher molecular size and weight. At highest concentration of 2000 mg/l (Fig. 1d), inhibition efficiency for HPMC is higher than HEC at 1st and 2nd day but waned at the 3rd day. The reason could be that HPMC has too high a viscosity which may have retarded molecular mobility. As a result could not diffuse properly onto the metal surface for adsorption, leading to lower inhibition whose decreasing effect is conspicuous beyond the third day of exposure (i.e at time, t > 3).

Another plausible explanation is that when a polymer is added to a given solvent, attraction as well as dispersion forces begin acting between its segments, according to their polarity, chemical characteristics, and solubility parameter. If the polymer-solvent interactions are higher than the polymer-polymer attraction forces, the chain segment start to absorb solvent molecules, increasing the volume of the polymer matrix, and consequently uncoil from their coiled shape. When this happens we say the segments are "solvated" instead of "aggregated" as they were in the solid state. The whole "solvation-unfolding-swelling" process takes a long time, and it is influenced only by the polymer-solvent interactions. For HPMC with such high concentration of 2000 mg/l, the reverse experience could be the case resulting to decreasing molecular adsorption on the metal surface.

Table 1. Calculated values of corrosion rate (mm/y) and inhibition efficiency (I.E.%) for mild steel corrosion in 1 M HCl in the absence and presence of different concentrations of HEC and HPMC from weight loss measurements

| HEC system	Corrosion rate (mm/y)					Inhibition efficiency (I.E. %)				
	Day 1	Day 2	Day 3	Day 4	Day 5	Day 1	Day 2	Day 3	Day 4	Day 5
Blank	0.84	0.45	0.37	0.30	0.24	-	-	-	-	-
500 mg/L	0.66	0.34	0.25	0.19	0.16	20.81	21.77	32.83	34.04	34.11
1000 mg/L	0.48	0.25	0.17	0.14	0.14	39.93	41.96	52.13	52.25	39.49
1500 mg/L	0.12	0.06	0.05	0.04	0.05	86.24	86.44	87.22	87.23	79.21
2000 mg/L	0.15	0.08	0.04	0.03	0.03	83.56	82.33	90.98	89.84	89.49
HPMC system	Day 1	Day 2	Day 3	Day 4	Day 5	Day 1	Day 2	Day 3	Day 4	Day 5
Blank	0.84	0.45	0.37	0.30	0.24	-	-	-	-	-
500 mg/L	0.12	0.07	0.05	0.04	0.03	84.56	84.86	86.72	86.76	86.45
1000 mg/L	0.10	0.06	0.04	0.04	0.03	86.58	86.75	87.22	87.00	87.38
1500 mg/L	0.09	0.05	0.04	0.03	0.03	88.59	88.64	89.72	89.84	88.55
2000 mg/L	0.12	0.05	0.03	0.04	0.03	85.24	87.38	90.48	86.05	86.22
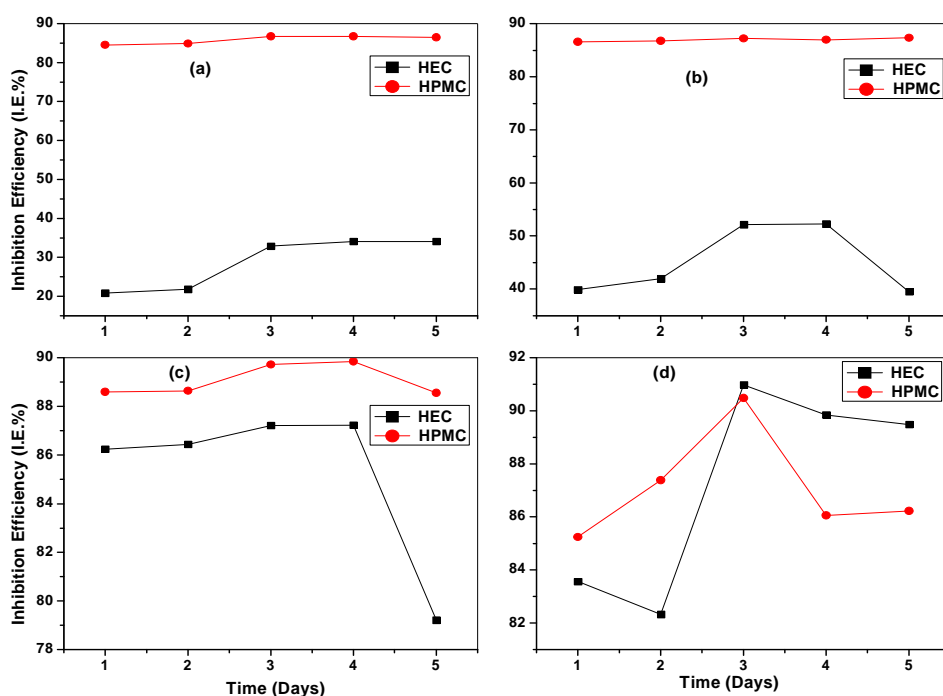
Fig. 1. Comparative effect of HEC and HPMC on mild steel corrosion inhibition in 1 M HCl against time at different inhibitor concentrations: (a) = 500 mg/l; (b) = 1000 mg/l; (c) = 1500 mg/l; (d) = 2000 mg/l

3.2 Impedance Results of the Polymeric Film

EIS provides a rapid and convenient way to evaluate the performance of organic-coated metals and has been widely used for investigation of protective properties of organic inhibitors on metals. It does not disturb the layer at the metal/solution interface. Therefore more reliable results can be obtained from this technique. Nyquist plots for mild steel in 1 M HCl solution containing 2000 mg/l of the HEC and HPMC as well as KI have been given in Fig. 2 (a). It is clear from this Figure that in uninhibited solution, Nyquist plots yielded a slightly depressed semi-circle with only one – time constant. The depressed dispersion has been attributed to roughness and other inhomogeneities of the solid electrode. This indicates the corrosion of mild steel in 1 M HCl solution in the absence of inhibitor which is mainly controlled by a charge transfer process. In this case, the mild steel corrosion could only take place on the free surface of the metal and/or

within the pores. If the metal surface is fully covered, the corrosive species, i.e. dissolved oxygen, chloride ions, must diffuse along these pores to interact with the metal surface for corrosion to occur [28]. In the evaluation of Nyquist plots, the difference in real impedance at lower and higher frequencies is commonly considered as a charge transfer resistance, R_{ct}. The charge transfer resistance must also be corresponding to the resistance between the metal and the outer Helmholtz plane (OHP) [29]. The contribution of all resistances corresponding to the metal/solution interface, i.e. charge transfer resistance, diffuse layer resistance, accumulation resistance, film resistance, among others must be taken into account. Addition of HEC and HPMC to the corrodent solution did not lead to change of shape of impedance diagrams but in size. The observed increase in the impedance parameters in inhibited solutions is associated with the corrosion inhibiting effect of HEC and HPMC. A depressed capacitive semicircular loop at high frequency region was attributed to the charge transfer resistance and

5

the diffuse layer resistance. Further observation of Fig. 2 (a) shows higher adsorption of HPMC than HEC as shown by the larger value of R_{ct}, which is a confirmation of the result demonstrated by the weight loss measurements. As seen from the Fig. 2 (a) also, R_{ct} values increased with addition of KI to HEC and HPMC respectively, which can be attributed to the formation of a more protective film layer at the metal surface, which increased the barrier for the mass and charge transfers. In contrast to the sole behavior of HEC, and HPMC, HEC showed better co-operative effect with KI than HPMC, a behavior which may be attributed to the better interaction between HEC^+ and I^- than $HPMC^+$ and I^-.

The inhibition efficiency is calculated from the relationship shown in equation (3):

$$I.E.\% = \left\{1 - \frac{Ctr}{Ctr_{inh}}\right\} X100 \qquad (3)$$

where C_{tr} and C_{trinh} are the charge transfer resistances without and with addition of inhibitor respectively. The values of the impedance data are listed in Table 2.

3.3 Potentiodynamic Polarization Results

Fig. 2 (b) presents the anodic and cathodic polarization curves of mild steel in 1 M HCl solution in the absence and presence of HEC, HPMC, HEC+KI and HPMC+KI respectively.

From the polarization curves, it could be observed that the corrosion potential remains almost constant in the presence of the inhibiting systems. The presence of the inhibitor systems caused a clear decrease in the cathodic current densities, probably due to the adsorption of the organic inhibitor systems at the active sites of the metal surface, suppressing the hydrogen evolution reaction and consequently slowing the corrosion rates. In the anodic domain, there is decrease in the current densities with increase in the corrosion potential up to a certain critical point, -0.35 V, beyond which the effect of anodic partial inhibitive reaction diminished with increasing corrosion potential. It is important to note that at the anodic domain, two distinct regions are conspicuous which are defined by the stated corrosion potential. Below this value, there is inhibition, whereas above the corrosion potential (-0.35 V), the additive obviously interfered with the stability of the adsorbed film, rendering it less protective, with resultant escalation of the anodic current density. The additives therefore exerted an inhibiting effect in cathodic domain and the anodic domain below the corrosion potential of -0.35 V. These regions are thus responsible for the overall inhibiting effect of the additives as corroborated by weight loss and impedance measurements. The anodic domain above the corrosion potential of -0.35 V exerted a corrosion stimulating effect on the anodic partial reaction, suggesting that part of the anodic corrosion reaction is the predominant reaction determining the corrosion rate of the system.
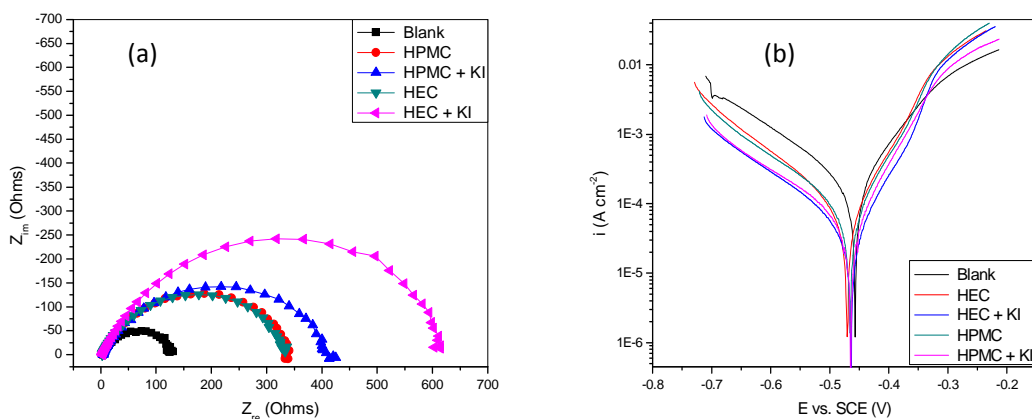

Fig. 2.(a) Nyquist impedance plots and (b) Polarization curves, of mild steel corrosion in 1 M HCl for HEC and HPMC, in the absence and presence of KI
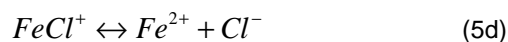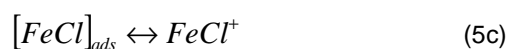
In general, it could be said that polarization results have aptly highlighted the complexities of the processes associated with the corrosion and corrosion inhibition of mild steel in hydrochloric acid. For instance, from point of view of corrosion inhibition performance, it could be reasoned that the reaction of HCl with Fe from mild steel may result in the formation of passive oxide film. This interferes with (or actually restricts) bulk adsorption of HEC and HPMC under the prevailing experimental conditions, thereby limiting the inhibiting effect to more cathodic potentials and anodic potentials below -0.35 V where the absence of oxide film would allow the formation of protective polymeric films of HEC and HPMC.

3.4 Adsorption and Thermodynamic Considerations

Functional polymers are characterized by multiple reactive centres (functional groups) which enable them to undergo multiple reactions in a system. The adsorption of cellulosic polymers (HEC and HPMC) on the mild steel surface may have occurred directly via donor-acceptor interactions between the free pair electrons of the glucosidic ring and oxygen atoms of the cellulosic polymers and the vacant d-orbitals of mild steel surface atoms. The polymers may have been adsorbed on the mild steel surface in the form of neutral molecules involving the substitution of pre-adsorbed water molecules from the metal surface and sharing of electrons between the oxygen atoms of the glucosidic ring and the mild steel surface.

$$Inh_{(sol)} + xH_2O_{(ads)} \leftrightarrow Inh_{(ads)} + xH_2O_{(sol)} \quad (4)$$
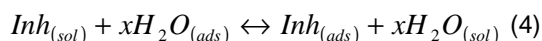
where x represents the number of water molecules replaced by one molecule of adsorbed inhibitor. Thus, the metal surface is efficiently isolated from the corrosive medium. In acid solutions in particular, the majority of organic compounds do exist as protonated species and others in the molecular form. The mode of adsorption of protonated molecules of the HEC and HPMC on mild steel surface can follow the proposed reaction sequence of mild steel corrosion in hydrochloric acid reported by [30]:

$$Fe + Cl^- \leftrightarrow [FeCl^-]_{ads} \quad (5a)$$

$$[FeCl^-]_{ads} \leftrightarrow [FeCl]_{ads} + e^- \quad (5b)$$

$$[FeCl]_{ads} \leftrightarrow FeCl^+ \quad (5c)$$

$$FeCl^+ \leftrightarrow Fe^{2+} + Cl^- \quad (5d)$$

It is an acceptable fact that chloride ions have a small degree of hydration, and due to specific adsorption, they should be first adsorbed on the positively charged metal surface. The adsorption of chloride ions creates an excess negative charge towards the solution side of metal (Eqn. 5a) and favors more adsorption of cations (i.e protonated molecules of HEC and HPMC) [31].

In strong acid solutions, the inhibitor molecules are expected to be protonated (Eqn. 6a) in equilibrium with the corresponding neutral form. Consequently, we have

$$Inh + H^+ \rightarrow InhH^+ \quad (6a)$$

$$[FeCl^-] + InhH^+ \rightarrow [FeCl^- InhH^+]_{ads} \quad (6b)$$
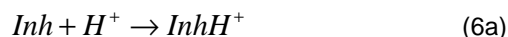
Then, the inhibitor molecules adsorb through electrostatic interactions between the negatively charged metal surface and positively charged inhibitor molecules of HEC and HPMC and form a protective metal-inhibitor barrier complex of adsorption film $[FeCl^- InhH^+]_{ads}$ (Eqn. 6b). By this, the oxidation reactions (Eqns. 5 c and d) can be prevented. In a similar reaction pattern, protonated molecules of HEC and HPMC can electrostatically interact with species, and then the oxidation of $[FeCl^-]_{ads}$ to $[FeCl]_{ads}$ (Eqn. 5b) can be prevented as well.

In order to understand the nature and modes of adsorption of HEC and HPMC inhibitors on the corroding mild steel surface, the surface coverage (θ) values and inhibitor concentrations (C) obtained from the weight loss measurements are fitted into the adsorption isotherm of the Thermodynamic-Kinetic model of El-Awady et al. [32] given by the expression

$$\log\left[\frac{\theta}{1-\theta}\right] = \log K^i + y \log C \quad (7)$$

θ and C retain their previous meanings. K_{ads} is the equilibrium constant of adsorption and $K_{ads} = K^{i \ 1/y}$. Here, 1/y is the number of active sites occupied by one molecule of inhibitor (or

the number of water molecules replaced by one molecule of inhibitor). The plot of $\log\left[\dfrac{\theta}{1-\theta}\right]$ against $\log C$ gives a straight line which approximate to El-Awady model as shown in Fig. 3.

The data obtained from the plot are given in Table 3. In the Table 3, the value of 1/y obtained shows that HEC molecule gives values less than 1 which indicate that one molecule of HEC could not block completely one active site on the corroding mild steel surface. On the other hand, HPMC molecule gives values greater than unity indicating that one molecule of HPMC occupies more than one active site on the mild steel surface, covering larger surface area. This confirms the higher inhibition efficiency of HPMC than HEC occasioned by its higher molecular weight.

In general, K_{ads} represents the adsorption power of the inhibitor molecule on the metal surface. The positive values confirm the adsorbability of HEC and HPMC on the mild steel surface. However, at the 4th and 5th day, K_{ads} values are too large to be accommodated. The free energy of adsorption (ΔG_{ads}) obtained from Eqn. (8) which is evaluated from K_{ads} is also given in Table 3:

$$\Delta G_{ads} = -RT \ln\left(55.5 K_{ads}\right) \qquad (8)$$

where R and T are the universal gas constant and absolute temperature, respectively. The negative ΔG_{ads} values imply that the adsorption of HEC and HPMC on the mild steel surface was favourable from thermodynamics point of view. The values of standard free energy of adsorption, ΔG_{ads} obtained indicated pure physical adsorption of the HEC inhibiting molecules, whereas HPMC molecules exhibited intrinsic propensity towards chemical adsorption on the mild steel surface. This definition is made on the basis of accepted values of standard adsorption free energy of -20 kJ mol^{-1} or less negative being associated with an electrostatic interaction between charged molecules and charged metal surface which indicate physical adsorption; and those of -40 kJ mol^{-1} or more negative involving charge sharing or transfer from the inhibitor molecules to the metal surface to form a co-ordinate covalent bond which is suggestive of chemical adsorption [33].

3.5 Effect of KI Addition

The addition of halide ions to inhibitor systems has been found to either inhibit or stimulate corrosion reaction of metals in acid solutions [34]. In most cases, halide ions are known to enhance adsorption of organic cation-type inhibitors in solution by forming intermediate bridges between the metal surface and the organic inhibitor. Accordingly, impedance and polarization tests undertaken discussed the cooperative (or synergistic) effect of KI with HEC and HPMC as illustrated in Fig. 2. Impedance results show that KI addition further increased the adsorption of HEC and HPMC on the mild steel surface. This is attributed to stabilization of the adsorbed inhibitor on the mild steel surface caused by the interaction between HEC^{+} and I- or HPMC^{+} and I-, which leads to more surface coverage. Thus, an improvement of inhibition efficiency on addition of KI is an indication of the participation of protonated inhibitor species in the adsorption process. In a similar vein, addition of KI caused reduction of cathodic corrosion current density and anodic corrosion current density up to the corrosion potential of -0.35 V. Beyond this potential, KI interferes with the passive film and stimulates anodic corrosion. This is due to the well-known adverse effect of halogens on passivity [17,26].

3.6 Quantum Chemical Computation

One molecule each of HEC and HPMC structures were first subjected to Forcite geometry optimization using condensed phase optimized molecular potentials for atomistic simulation studies (COMPASS) force field and the Smart minimized method by high-convergence criteria [35]. The electronic structures of HEC and HPMC were well determined, including the distribution of frontier molecular orbitals with a view to establishing the active sites of the molecules. The simulations were performed by means of the density functional theory (DFT) electronic structure program, DMol^{3} using a Mulliken population analysis. Electronic parameters for the simulation include restricted spin polarization using the DND basis set and the Perdew Wang (PW) local correlation density functional. According to the frontier molecular orbital (FMO) theory of chemical reactivity, transition of electrons is due to an interaction between the HOMO and the LUMO of the reacting species. The HOMO energy (E_{HOMO}) characterizes the susceptibility of the molecule towards the attack by electrophiles,

where high values E_{HOMO} indicate a tendency of the molecule to donate electrons to an appropriate acceptor molecule with low energy or an empty electron orbital, in the case of mild steel metal. The energy of LUMO is associated the susceptibility of molecules towards nucleophilic attack. Fig. 4 illustrates the geometry optimized structure, HOMO and LUMO orbitals of HEC and HPMC. The regions of highest electron density represent the active centres with the greatest ability to donate electron pairs and hence attach to the metal surface. It is clear that the HOMO of HEC and HPMC is distributed almost exclusively around the glucosidic ring and oxygen atoms with evidence of an electron delocalization region. Again, the low values of the energy gap ΔE means that the energy to remove an electron from the last occupied orbital is minimized, implying good inhibition efficiency [36]. The values of E_{HOMO} and E_{LUMO} are -5.589 and -0.139 eV respectively for HEC whereas -0.352 eV (E_{HOMO}) and 0.313 (E_{LUMO}) eV are for HPMC. The energy gap of the HEC and HPMC molecules are 5.450 and 0.665 eV respectively. These results show that HPMC has lower energy gap than HEC, suggesting that HPMC should possess better inhibitive capability than HEC.

3.7 Molecular Dynamics (MD) Simulation

Molecular dynamics simulation was also undertaken to illustrate the physical movement of atoms and molecules of the inhibitor on the metal surface during adsorption process. MD simulation of the interaction between a single molecule of HEC or HPMC molecule and mild steel surface was performed using Forcite quench molecular dynamics in the MS modeling 4.0 software to sample many different low energy minima and to determine the global energy minimum. Calculations were carried out in a 12 x 8 supercell using the COMPASS force field and Smart algorithm. The Fe which represents mild steel crystal was cleaved along the (1 1 0) plane. Fig. 5 presents the optimized (low energy)

adsorption model for a single molecule of HEC (a) and HPMC (b) on the Fe (1 1 0) surface from from our simulation. The effects of solvent and charge are equivalent and their cancel out. In compliance with the results of the electronic distribution model (Frontier molecular orbital), HEC and HPMC molecules adsorb on the mild steel surface via the glucosidic ring and the oxygen atoms, with a somewhat lateral orientation. This is possible due to outstanding binding energy between the inhibiting molecule and the metal surface. It is pertinent to note here the essence of binding energy which is a measure of the energy required to free electrons from their atomic orbitals. On the other hand, binding energy represents the mechanical energy that must be done against the forces which hold an inhibiting molecule together, disassembling the inhibiting molecule into their component parts. The binding energies between the HEC and Fe surface, and HPMC and Fe surface were found to be -119.5 eV and -114.0 eV respectively using the following equation [37]:

$$E_{binding} = E_{Total} - [E_{Inhibitor} + E_{Fe}] \quad (9)$$

From the binding energy ($E_{binding}$) results, it is therefore evident that HPMC molecule/Fe surface has higher $E_{binding}$ than HEC/Fe surface. This implies that HPMC/Fe possessed stronger interact bonds and requires higher energy to break. However, the overall adsorption process of the inhibiting molecules and the consequent corrosion inhibition is still governed by adsorption period. If inhibiting molecules are allowed to exhaust their bulk adsorption process, higher molecular weight compounds will ultimately give better corrosion inhibition than their lower molecular weight counterparts. This is in agreement with the experimental results presented in Fig. 2 except where the system is influenced by limited immersion period and incorporation of co-additives which may alter the original reaction kinetics.

Table 2. Impedance and polarization parameters and corresponding inhibition efficiency for corrosion of mild steel in 1 M HCl in the presence and absence of KI for (a) HEC and (b) HPMC

System	R_{ct} (Ω)	n	I.E. %	E_{corr} (mV(SCE))	I_{corr} (µA cm^{-2})	R_p (Ω cm^2)
(a)Blank	125.1	0.8297	-	-481.29	74.893	396.03
HEC	336.4	0.8024	62.81	-470.78	66.054	329.11
HEC + KI	650.4	0.7794	80.77	-463.64	33.263	653.56
(b)Blank	125.1	0.8297	-	-481.29	74.893	396.03
HPMC	347.3	0.7841	63.98	-465.98	65.403	322.53
HPMC +KI	413.7	0.7768	69.76	-464.62	42.017	517.39

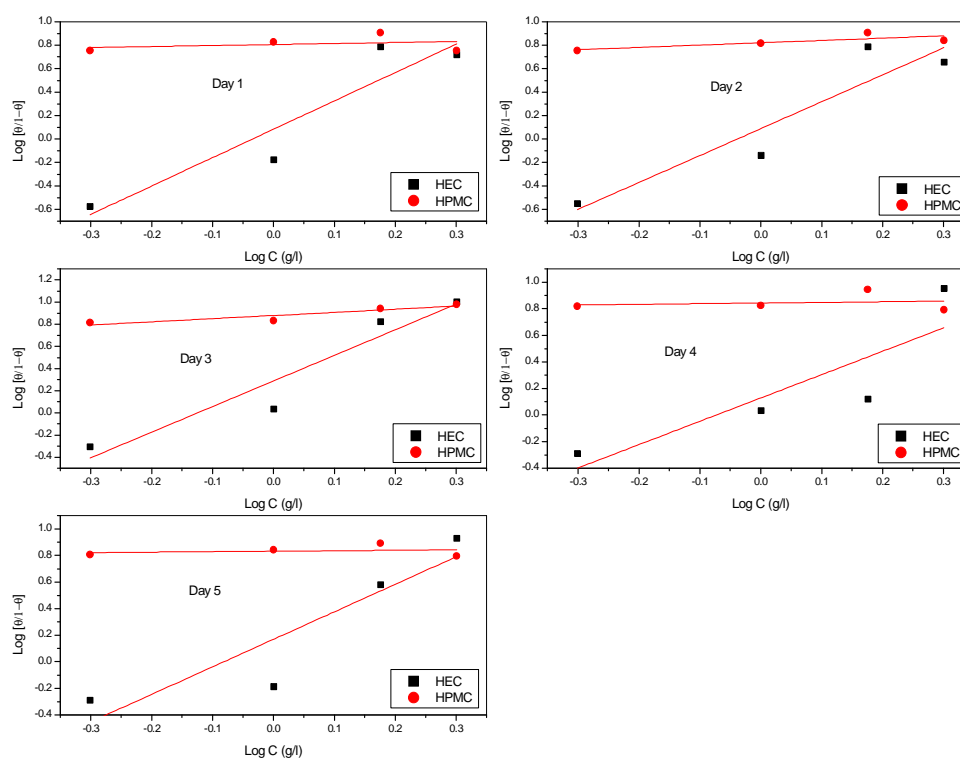**Fig. 3. Plots of Thermodynamic-Kinetic model for mild steel corrosion in 1.0 M HCl in the presence of HEC and HPMC under atmospheric condition**

3.8 Influence of Molecular Weight on Inhibition Performance of HPMC and HEC

The size of polymer molecules may sometimes be expressed in terms of its molecular weight. The molecular weight affects the viscosity and chain mobility of polymer molecules. The use of polymers as corrosion inhibitors particularly in the aqueous state exhibits a lot of interaction differentials with respect to its molecular weight. HEC and HPMC used in this study have displayed good corrosion inhibition performance. However, it is important also to ascertain the influence of their bulk molecular weight property on the inhibition performance of mild steel corrosion in HCl medium. The values in Table 4 have been extracted from the results of experimental data, to compare the net inhibitive effect of HEC and HPMC.

The weight loss and EIS results showed that HPMC exhibited better inhibition performance. Potentiodynamic polarization reveals that HPMC has lower corrosion current density meaning that HPMC/mild steel interface showed lower tendencies to corrosion than HEC/mild steel interface. On the basis of molecular orbital, high values of E_{HOMO} indicate the tendency of the molecules to donate electrons to an appropriate acceptor with vacant molecular orbitals. Therefore, HPMC showed better disposition than HEC.

On the other hand, low values of energy gap indicate higher reactivity of the molecule with respect to adsorption on the mild steel surface and therefore render good inhibition efficiency, since the energy to remove an electron from the least occupied orbital will be minimal. With respect to binding energy, HPMC molecule/Fe interface has higher $E_{binding}$ (-114.0 eV) than

HEC/Fe interface (-119.5 eV). This again validates the better inhibitive performance of HPMC than HEC on account of their molecular weight. 1/y values from adsorption isotherm seem to explain the number of active corrosion sites covered by one molecule of the inhibiting additive. The values reveal that one molecule of HPMC covered more corrosion sites than HEC did. This fact is also traceable to the bulk molecular weight. Recall that K_{ads} represents the adsorption strength of molecules, and showed that HPMC was better adsorbed on the metal surface than HEC. This authenticates the results from molecular orbitals and binding energy. The values of all these parameters have demonstrated that HPMC which has higher molecular weight was better strongly adsorbed on the corroding mild steel surface.

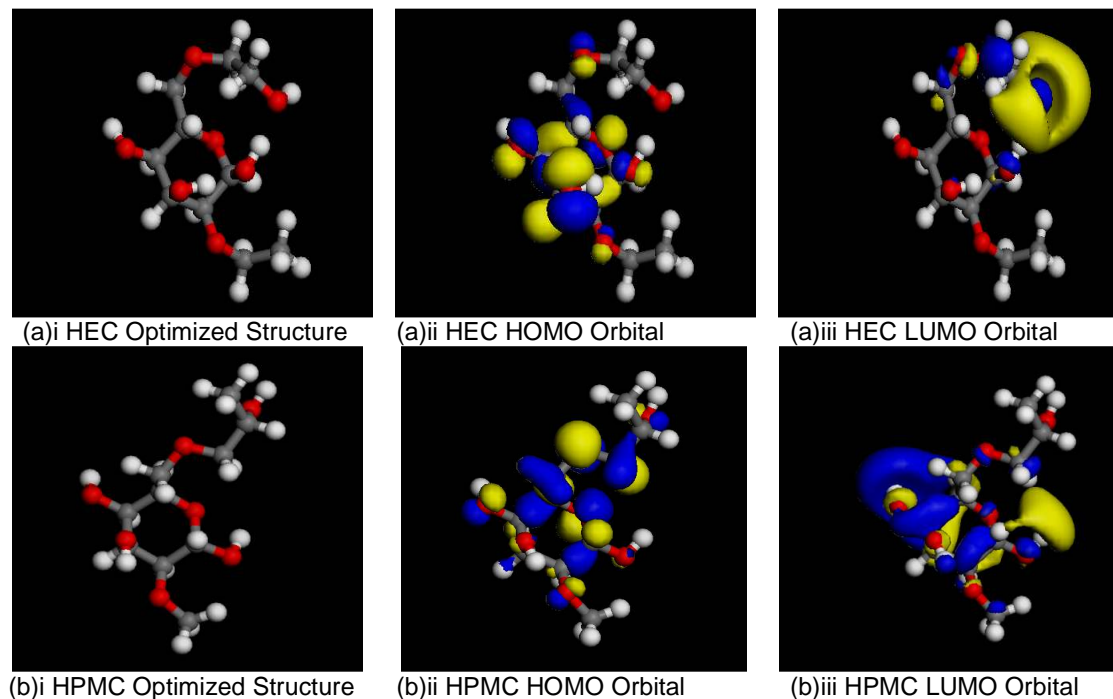| (a)i HEC Optimized Structure | (a)ii HEC HOMO Orbital | (a)iii HEC LUMO Orbital |
| (b)i HPMC Optimized Structure | (b)ii HPMC HOMO Orbital | (b)iii HPMC LUMO Orbital |

Fig. 4. Electronic properties of Hydroxyethyl cellulose (HEC) and Hydroxypropyl methylcellulose (HPMC) [C, grey; H, white; O, red]. The blue and yellow surfaces depict the electron density difference; the blue regions show electron accumulation, while the yellow regions show electron loss
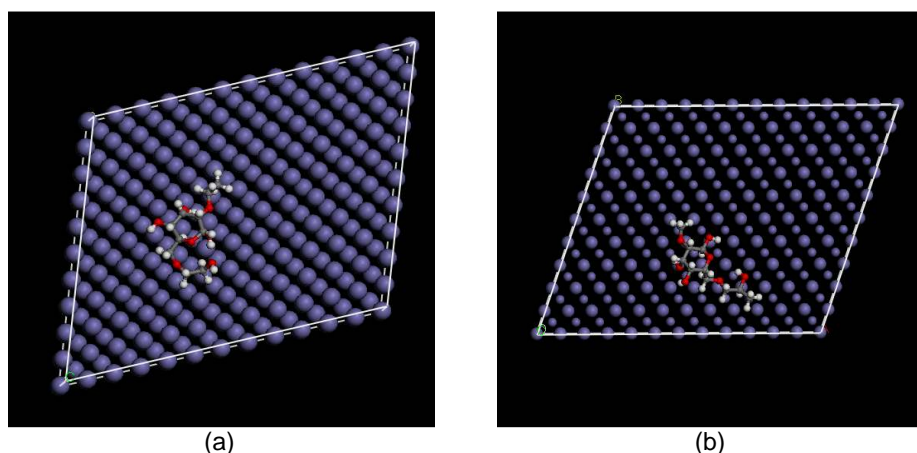
| (a) | (b) |

Fig. 5. Adsorption configurations of (a) HEC and (b) HPMC on Fe (1 1 0) surface showing the adsorption mode on the metal surface

Table 3. Adsorption parameters for Thermodynamic-Kinetic isotherm for mild steel corrosion in 1.0 M HCl in the presence of HEC and HPMC

Immersion period (Days)	Inhibitor	1/y	K^i	$K_{ads}=K^{i\ 1/y}$	ΔG_{ads}
1	HEC	0.4	1.211	1.082	-10.282
	HPMC	11.9	1.214	9.960	-15.886
2	HEC	0.4	1.225	1.093	-10.308
	HPMC	5.1	6.627	14953.9	-34.220
3	HEC	0.4	1.940	1.332	-10.804
	HPMC	3.5	7.568	1224.2	-27.937
4	HEC	0.6	1.344	1.183	-10.506
	HPMC	21.0	6.969	∞	-
5	HEC	0.5	1.474	1.206	-10.555
	HPMC	30.2	6.797	∞	-

Table 4. Some extracted values to illustrate the influence of molecular weight on corrosion inhibition

Parameters Molecule	IE% (Weight Loss)		IE% (EIS)	I_{corr} (PDP)	E_{HOMO} (eV)	E_{LUMO} (eV)	ΔE (eV)	$E_{binding}$ (eV)	Adsorption parameters (days 1 and 2)			
	500 mg/l	1000 mg/l							1/y		K_{ads}	
HEC	34.11	39.49	62.81	66.054	-5.589	-0.139	5.450	-119.5	0.40	0.40	1.082	1.093
HPMC	86.45	87.38	63.98	65.403	-0.352	0.313	0.665	-114.0	11.9	5.1	9.960	14953.9

4. CONCLUSION

In view of the experimental and theoretical results of the study undertaken, HPMC shows better inhibitive capability than HEC in 1 M HCl medium, on account of its larger molecular weight and size. Weight loss measurements results reveal higher inhibition efficiency values for HPMC than HEC at 500, 1000 and 1500 mg/l but shows decreasing value at 2000 mg/l, possibly due to the high viscosity which may have retarded the molecular mobility. Impedance results show better adsorption of HPMC than HEC which follow the Thermodynamic-Kinetic adsorption model of El-Awady et al. Polarization measurements indicate that HPMC has lower values of corrosion current density than HEC. However, the two inhibitors have proven to be of mixed-type with predominant cathodic effect. Quantum chemical parameters obtained showed that HPMC has better susceptibility to donate electrons and interact with mild steel surface. Also from the frontier molecular orbital theory, the active region responsible for the adsorption of the inhibitors is located around the oxygen atoms and the glucosidic ring of the molecules. In summary, it can be deduced that the inhibitive effectiveness of HPMC molecule is better than HEC due largely to the higher molecular weight and size.

COMPETING INTERESTS

Authors have declared that no competing interests exist.

REFERENCES

1. Shukla SK, Singh AK, Quraishi MA. Triazines: Efficient corrosion inhibitors for mild steel in hydrochloric acid solution. Int. J. Electrochem. Sci. 2012;7:3371–3389.

2. Vasudha VG, Shanmuga Priya K. *Polyalthia longifolia* as a corrosion inhibitor for mild steel in HCl solution. Research Journal of Chemical Sciences. 2013;3(1): 21-26.

3. Oguzie EE, Li Y, Wang SG, Wang F. Understanding corrosion inhibition mechanisms – Experimental and theoretical approach. RSC Adv. 2011;1: 866–873.

4. Vishnudevan M. Mitigation of mild steel corrosion in acidic solution using inhibitor. E-Journal of Chemistry. 2011;8(S1):S53-S60.

5. Saratha R, Vasudha VG. Emblica officinalis (Indian Gooseberry) leaves extract as corrosion inhibitor for mild steel in 1N HCl. E-Journal of Chemistry. 2010; 7(3):677-684.

6. Arukalam IO, Ijomah NT, Nwanonenyi SC, Obasi HC, Aharanwa BC, Anyanwu PI. Studies on acid corrosion of aluminium by a naturally occurring polymer (Xanthan gum). International Journal of Scientific & Engineering Research. 2014;5(3):663-673.

7. Arukalam IO, Alaohuru CO, Ugbo CO, Jideofor KN, Ehirim PN, Madufor IC. Effect of Xanthan gum on the corrosion protection of aluminium in HCl medium. International Journal of Advancements in Research & Technology. 2014;3(3):5-16.

8. Kumar A, Sankar A, Kumaravel M, Rameshkumar S. Clitoria Ternatea-extracts as corrosion inhibitor for mild steel in acid medium. International Journal of Engineering Research and Development. 2013;5:64-67.

9. Arukalam IO, Madufor IC, Ogbobe O, Oguzie EE. Inhibition of mild steel corrosion in sulfuric acid medium by hydroxyethyl cellulose. Chemical Engineering Communications. 2015; 202(1):112-122.

10. Frignani A, Tommesani L, Brunoro G, Monticelli C, Fogagnolo M. Influence of the alkyl chain on the protective effects of 1,2,3-benzotriazole copper corrosion. Corros. Sci. 1999;41:1205.

11. Umoren SA. Polymers as corrosion inhibitors for metals in different media– A review. The Open Corrosion Journal. 2009; 2:175–188.

12. Arthur DA, Jonathan A, Ameh PO, Anya C. A review on the assess-ment of polymeric materials used as corrosion inhibitor of metals and alloys. International Journal of Industrial Chemistry. 2013;4(2):1–9.

13. Satapathy AK, Gunasekaran G, Sahoo SC, Amit K, Rodrigues PV. Corrosion inhibition by *Justica gendarussa* plant in hydrochloric acid solution. Corros. Sci. 2009;51:2848-2856.

14. Oguzie EE, Akalezi CO, Enenebeaku CK, Aneke JN. Corrosion inhibition and adsorption behavior of malachite green dye on aluminum corrosion. Chem. Eng. Commun. 2011;198(1):46–60.

15. Arukalam IO, Madufor IC, Ogbobe O, Oguzie EE. acidic corrosion inhibition of copper by hydroxyethyl cellulose. British Journal of Applied Science and Technology. 2014;4(9):1445-1460.

16. Arukalam IO, Madufor IC, Ogbobe O, Oguzie E. Experimental and theoretical studies of hydroxyethyl cellulose as inhibitor for acid corrosion inhibition of mild

17. Arukalam IO, Madufor IC, Ogbobe O, Oguzie EE. Hydroxypropyl methylcellulose as a polymeric corrosion inhibitor for aluminium. Pigment and Resin Technology. 2014;43(3):151-158.

18. Chidiebere MA, Ogukwe CE, Oguzie KL, Eneh CN, Oguzie EE. Corrosion inhibition and adsorption behaviour of Punica granatum extract on mild steel in acidic environments: Experimental and theoretical studies. Ind. Engrg. Chem. Research. 2012;51:668-677.

19. Quraishi MA, Singh A, Singh VK, Yadav DK, Singh AK. Green approach to corrosion inhibition of mild steel in hydrochloric acid and sulphuric acid solutions by the extract of Murraya koenigii leaves. Mater. Chem. & Phys. 2010; 122:114-122.

20. Hansen C. Hansen solubility parameters: A user's handbook, second edition, Boca Raton, Fla: CRC press; 2007. ISBN: 978-0-8493-7248-3.

21. Vastag Gy, Szöcs E, Shaban A, Kálmán E. New inhibitors for copper corrosion. Pure Appl. Chem. 2001;73(12):1861–1869.

22. Mazen MK. The effect of molecular weight on corrosion protection properties of polyvinyl pyrrolidone polymers on stainless steel. Arab J Sci Eng. 2007;35(1A):29–39.

23. Yurt A, Butun V, Duran B. Effect of the molecular weight and structure of some novel water soluble triblock copolymers on the electrochemical behaviour of mild steel. Mater Chem Phys. 2007;105:114–121.

24. Kumar A, Sankar A, Kumaravel M, Rameshkumar S. Clitoria Ternatea-extracts as corrosion inhibitor for mild steel in acid medium. International Journal of Engineering Research and Development. 2013;5:64-67.

25. Mani Megalai S, Ramesh R, Manjula P. Inhibition of corrosion mild steel in acid media by trazodone drug. Research Desk. 2013;2(4):326-333.

26. Arukalam IO, Madu IO, Ijomah NT, Ewulonu CM, Onyeagoro GN. Acid corrosion inhibition and adsorption behaviour of Ethyl hydroxyethylcellulose on mild steel corrosion. Journal of Materials. 2014;1-11.
Available:http://dx.doi.org/10.1155/2014/101709

27. Liu J, Yu W, Zhang J, Hu S, You L, Qiao G. Molecular modeling study on inhibition performance of imidazoline for mild steel in CO_2 corrosion. Applied Surface Science. 2010;256:4729-4733.

28. Oguzie EE, Unaegbu C, Ogukwe CN, Okolue BN, Onuchukwu AI. Inhibition of mild steel corrosion in sulphuric acid using indigo dye and synergistic halide additives. Materials Chemistry and Physics. 2004; 84:363-368.

29. Lebrini M, Robert F, Vezin H, Roos C. Electrochemical and quantum chemical studies of some indole derivatives as corrosion inhibitors for C38 steel in molar hydrochloric acid. Corros Sci. 2010;52: 3367-3376.

30. Oguzie EE, Enenebeaku CK, Akalezi CO, Okoro SC, Ayuk AA, Ejike EN. Adsorption and corrosion-inhibiting effect of Dacryodis edulis extract on low-carbon-steel corrosion in acidic media. Journal of Colloid and Interface Science. 2010;349: 283-292.

31. Amin MA, Ibrahim MM. Corrosion and corrosion control of mild steel in concentrated H_2SO_4 solutions by a newly synthe-sized glycine derivative. Corrosion Sci. 2011;53:873-885.

32. Kissi M, Bouklah M, Hammouti B, Benkaddour M. Establishment of equivalent circuits from electrochemical impedance spectroscopy study of corrosion inhibition of steel by pyrazine in sulphuric acidic solution. Appl. Surf. Sci. 2006;252:4190-4197.

33. Ashassi-Sorkhabi H, Seifzadeh D, Hosseini MG. EN, EIS and polarization studies to evaluate the inhibition effect of 3H-Phenothiazin-3-one, 7-dimethylamin on mild steel corrosion in 1 M HCl solution. Corros. Sci. 2008;50:3363-3370.

34. Oguzie EE. Inhibition of acid corrosion of mild steel by *Telfaria occidentalis* extract. Pigment & Resin Technology. 2005;34(6): 321-326.

35. Issa RM, Awad MK, Atlam FM. Quantum chemical studies on the inhibition of corrosion of copper surface by substituted uracils. Applied Surface & Science. 2008; 255:2433-2441.

36. Rodriguez-Valdez LM, Martinez-Villafane LM, Glossman-Mitnik D. Computational simulations of the molecular structure and properties of heterocyclic organic compounds with possible corrosion inhibition properties. J. Mol. Struct. Theochem. 2005;713:65-70.

37. Bartley J, Huynh N, Bottle SE, Flitt H, Notoya T, Schweinsberg DP. Computer simulation of the corrosion of copper in acidic solution by alkyl esters of 5-carboxybenzotriazole. Corros. Sci. 2003; 45:81-96.

_____

Peer-review history:
The peer review history for this paper can be accessed here:
http://sciencedomain.org/review-history/12097